A validated CFD model of plain and serrated fin-tube bundles

Karl Lindqvist*, Erling Næss

Department of Energy and Process Engineering,
Norwegian University of Science and Technology, N-7491 Trondheim, Norway

Abstract

This work presents a Computational Fluid Dynamics model of helically wound fin tube bundles and demonstrates its predictive capability for thermal-hydraulic performance. A consistent validation against experimental data is given for four different fin tube geometries, two with plain fins and two with serrated fins. Predicted heat transfer and pressure drop data are within, or very close to, the experimental uncertainty, with maximum root mean square errors of 13.8 % and 14.4 % respectively. The modeled fin temperature distribution is used to evaluate three fin efficiency models, revealing that correction equations can be in significant error for tall plain fins. Three sets of semi-empirical correlations for Nusselt and Euler numbers are also evaluated, showing non-conservative predictions for several of the tested geometries. Results from the study confirm the efficacy of reduced domain modeling, whereby geometric periodicity of the heat exchanger array is exploited to reduce computational cost.

Keywords: Numerical modeling; CFD; serrated fin; plain fin; thermal-hydraulic correlations; fin efficiency

Full article at publisher: https://doi.org/10.1016/j.applthermaleng.2018.07.060

1. Introduction

Waste heat recovery is currently under consideration in the offshore oil- and gas industry to mitigate the high energy use on platforms. Weight- and volume minimization of the heat exchanger core is vital due to the lack of space on these installations. Earlier work has indicated that overall Waste Heat Recovery Unit (WHRU) skid weight can be reduced by bringing down the tube diameter [1], which calls for an extension of the validity range of existing thermal-hydraulic design correlations. It is also highly desirable to be able to validate the performance of a thermally optimized design by detailed numerical modeling, before investing in fabrication and experimental testing. Computational Fluid Dynamics (CFD) can supplement experimental measurements and provide additional insights in this endeavor, provided that models are thoroughly validated.

Numerical CFD models have thus far contributed both qualitatively and quantitatively to the thermal-hydraulic modeling of finned tubes. Qualitatively, by giving an understanding the local flow phenomena around finned tubes. Quantitatively, by enabling sensitivity studies which are very time consuming to study experimentally.

As will be shown in the following, the majority of earlier modeling efforts have focused on simulating plain fin tubes, tube bundles with few (<5) tube rows and/or annular fin tubes. Large diameter tubes (≥25.4 mm) have been prioritized. Industrial relevance, combined with the possibility to exploit geometrical symmetry while keeping model size moderate have likely been the reasons behind this focus. In contrast, compact offshore waste heat recovery units can be expected to use helically wound serrated fins with small diameter tubes [2]. Moreover, many studies have compared modeling results with empirical correlations as a means of model validation. This approach is insufficient if model data are to be treated on par with experimental data, due to the large spread in predictions between different correlations.

The dissertation by Mon [3] constitute one of the first application of CFD to finned tube bundles. 29 different tube bundles with plain annular fins were modeled in staggered and in-line configuration, all having four tube rows. Mon's CFD model was capable of describing intuitive, qualitative trends in overall heat transfer performance. The simulations were used to propose a correction to the VDI Heat Atlas correlation [4], although direct validation with experiments were lacking. In a consecutive paper, Mon and Gross [5] compared results for eight of the modeled tube bundles to a few literature correlations. Similar work has been presented in [6, 7, 8], of which only Pathak et al. compared modeling results with experimental data.

The research by McIlwain [9] has many similarities with the work of Mon. Qualitative flow features were used to improve the pressure loss coefficients in the HTFS2 correlation. Six tube rows were modeled in all cases and

*Corresponding author
Email address: karl.erik.lindqvist@ntnu.no (Karl Lindqvist)

plain annular fins were considered. Experimental data for four in-line tube bundles and one staggered tube bundle was used for model validation, with good, albeit somewhat inconsistent, results.

Torresi et al. [10] modeled the pressure drop over a single serrated finned tube row and subsequently implemented a porous region model for the analysis of a full Heat Recovery Steam Generator (HRSG). Benchmark results compared favorably to a corresponding simulation in a proprietary 1D pressure loss code, but no comparison with experiments were made.

McIlwain [11] simulated two different single row tube bundles with plain and serrated fins, respectively, in order to explain the higher pressure drop and heat transfer rate of serrated fins. The same author also simulated a serrated fin-tube in multi-row inline configurations and compared the resulting pressure drop to that predicted from an industrial correlation [12].

The thesis of Hofmann [13] and subsequent publications [14, 15] presented experimental measurements and numerical models of one plain- and two serrated fin-tube geometries. Modeled and measured Nusselt numbers and pressure drop coefficients matched with reasonable accuracy, but significant scatter was seen in the experimental data. Only one tube row was modeled numerically. A particular model simplification was evaluated and concluded to be acceptable, namely to model helically wound fins as annular (flat) fins. It should, however, be noted that the investigated geometries had a relatively low fin pitch, making them amenable to this simplification.

Lemouedda et al. [16] compared the heat transfer/ pressure drop trade-off of plain versus serrated fins in a three-row tube bundle and studied the effect of fin tip twist and the number of fin segments. The study only considered moderate Reynolds numbers ($1320 \leq Re_{d_o} \leq 5750$) and did not validate the model with experiments. Moreover, it is the only published study, to the authors knowledge, that neglect turbulence modeling altogether and assume laminar flow.

Ó Cléirigh and Smith [17] modeled the heat transfer and pressure drop of three finned tube geometries with varying degree of serration (from plain, through halfway serrated to fully serrated). They showed that CFD gives similar results as correlations over large range of Reynolds numbers. Neither this study showed validation with experiments.

Martinez et al. [18] presented a modeling approach where a small section of a finned tube bank is simulated with fully periodic boundary conditions. Nusselt numbers and friction factors were compared with two correlations with satisfactory agreement. Detailed flow field data were also compared to experimental measurements. The authors went on to perform similar modeling of a six-row tube bundle including inlet and outlet regions in a subsequent publication [19]. A major conclusion of this work was that velocity, temperature and turbulence fields indeed show periodic behavior after the third tube row and that a fully periodic model therefore is appropriate. The same six-row

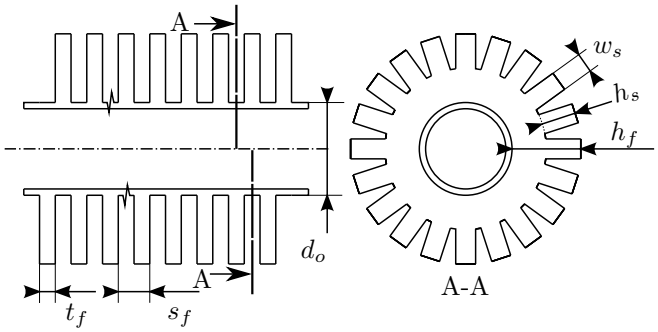

Figure 1: Fin tube geometric parameters

setup was finally used to show that a relatively large part of the fin can be removed without significantly affecting thermal-hydraulic performance [20].

In summary, only one publication (namely [9]) has validated simulations of more than one tube geometry, using a consistent numerical setup, with experimental data. This is troublesome, since an insufficient numerical setup or grid generation technique may seem acceptable for one particular geometry but break down in the general case. The validation case therefore needs to be revisited for helically wound fin tubes in staggered tube configurations, particularly for serrated fins. On a technical note, all but one publication make use of Reynolds averaging coupled with an eddy viscosity model of either k-ϵ or k-ω type. Due to the lack of validation, it is not clear at this point whether this modeling approach is sufficient or if higher fidelity modeling is needed.

The novelty of this study is firstly that the numerical model's predictive capabilities are demonstrated over a large range of tube- and fin dimensions. Consistent validation against experimental data for four rather different fin tube geometries from the literature is given. Secondly, the paper aims to evaluate the accuracy of fin efficiency correction equations, particularly for small diameter and high finned tubes. Fin efficiency corrections have received comparatively little attention in the literature, but can influence performance predictions significantly for non-standard fin tube geometries. A few selected thermal-hydraulic correlations are also discussed. The modeling approach and methods used in this paper are generally applicable for thermal-hydraulic performance estimation, particularly for heat exchangers with stream- and spanwise periodic geometry.

2. Fin tube geometries and semi-empirical equations

Four finned tube geometries from the literature are modeled in the present work, with geometric parameters given in Table 1 and depicted schematically in Figure 1. All geometries have previously been tested experimentally in multi-row staggered configurations in dedicated wind tunnels that are expected to be representative of conditions

Table 1: Tube and array geometries (cf. Figure 1 and Figure 2). All dimensions in mm unless stated.

Geometry	A	B	C	D
Reference	[21]	[22]	[23]	[24]
Fin type	plain	plain	serrated	serrated
Fin material	aluminum	copper	steel	steel
d_o [mm]	13.5	15.9	20.87	50.8
h_f [mm]	10	1.42	8.61	25.78
h_s [mm]			8.61	20.83
t_f [mm]	0.5	0.41	0.91	1.22
s_f [mm]	2.81	1.3	5.08	4.28
w_s [mm]			3.97	4.32
β^1 [deg]	30	30	30	30
c_f [mm]	5.2	8.8	8	11.94
P_t [mm]	38.7	27.5	46.1	114.3
P_l [mm]	33.5	23.9	39.9	99.0
h_f/r_o [-]	1.48	0.18	0.83	1.01
$h_f/\hat{s}_f$ [-]	4.33	1.60	2.06	8.42

[1]The tube bundle layout angle is defined as

$$\beta = \tan^{-1}\left(\frac{P_t}{2P_l}\right)$$

in a WHRU. Three sets of thermal-hydraulic correlations are used for reference, namely the mathematically simple PFR correlations [25], the industrially popular ESCOA correlations [26] and the recent correlations by Holfeld [21]. Relatively small diameter tubes are chosen to explicitly violate the validity ranges of the PFR and ESCOA correlations.

A measure of the uncertainty of the experimental data is necessary for a correct comparison with results from numerical modeling. Holfeld [21] reported uncertainties of 9.0–16.7 % for the Nusselt number and 25.2–4.3 % for the Euler number. The range corresponds to uncertainties at low Re and high Re, respectively. Næss [23] reported uncertainties of 4–8 % for Nusselt numbers and 10–2 % for Euler numbers. Since uncertainty analyses are missing in [24] and [22], we assume an approximate measurement uncertainty of 10 % for heat transfer and 15 % for pressure drop based on a review of other sources and taking all uncertainties (measured quantities, geometry, production standards, tube inside heat transfer) into account. These numbers also reflect the additional uncertainty in the Reynolds number.

Two correlations for fin efficiency correction are considered in this work, namely the Weierman correction [27],

$$\frac{\eta_f}{\eta_{f,\text{theo}}} = \begin{cases} 0.7 + 0.3\eta_{f,\text{theo}} & \text{Plain fin} \\ 0.9 + 0.1\eta_{f,\text{theo}} & \text{Serrated fin} \end{cases}$$

and the Hashizume correction [28],

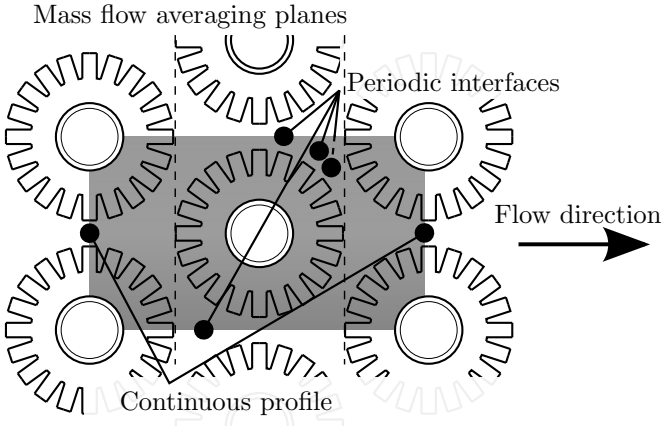

Figure 3: Reduced domain model setup

$$\frac{\eta_f}{\eta_{f,\text{theo}}} = 1 - (mh_f) \cdot \left(a + 0.14\left(\frac{d_o + 2h_f}{d_o}\right)^{2.7}\left(1 - 0.097\ln(\text{Re}_{d_o})\right)\right)$$

with

$$a = \begin{cases} 0 & \text{Plain fin} \\ 0.016\left(\frac{h_s}{w_s}\right) & \text{Serrated fin} \end{cases}$$

The theoretical fin efficiency is calculated based on the work of Hashizume et al. [28].

3. Numerical model

The numerical modeling approach in this paper is based on simulating a periodic "unit cell" in the heat exchanger array, building on the work of Martinez et al. [18] (cf. Figure 3). This approach reduces the computational cost considerably over modeling a full tube bundle. One of the tube geometries is also modeled in an eight row configuration (cf. Figure 2) to verify the efficacy of the reduced domain model. The common modeling assumptions are given in the following paragraphs.

3.1. Model equations and numerical setup

The steady Reynolds Averaged Navier-Stokes (RANS) equations are solved together with the energy equation and a model equation for turbulence using the open source CFD toolbox OpenFOAM v4.1. Second order upwind discretization is used for all convective terms. The Spalart-Allmaras turbulence model is selected due to its simplicity, robustness and suitability for simulating boundary layers under adverse pressure gradient conditions. It also yields similar results as other eddy viscosity turbulence models when applied to finned tube bundles [29]. All model constants were kept at their default value.

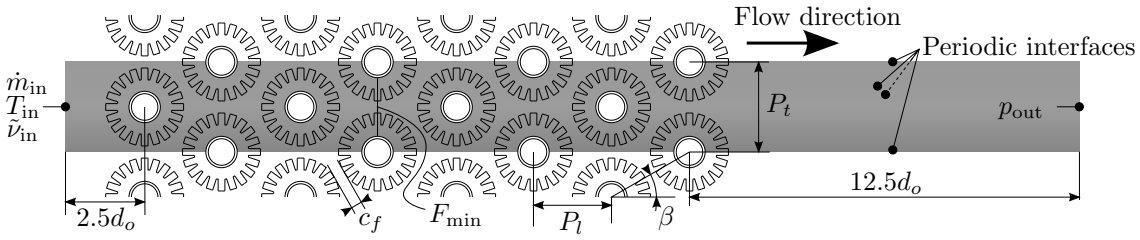

Figure 2: Computational domain, boundary conditions and array parameters; Full domain model

Turbulent viscosity is set to zero on solid wall surfaces, except for the fin tip and segment sides where wall functions for turbulent viscosity and turbulent thermal diffusivity are used. A turbulent Prandtl number of 0.85 is used throughout for thermal diffusivity calculations. The tube surface and the fin root is given a fixed temperature boundary condition of 298 K. Fin surfaces exposed to the fluid uses a coupled boundary condition with a consistent heat flux across the interface.

Two iterative convergence criteria are used: The drop in mass averaged total pressure ($p_0 + 0.5\rho U^2$) across the computational domain and the total surface heat flux from each fin surface. Equation residuals were also checked for monotonic reduction.

3.2. Thermophysical models

The fluid is modeled as dry air with constant thermophysical properties, including density. This simplification removes the dependency on whether the gas is cooled or heated by the tubes and is justified by the fact that the gas temperature change for each tube row usually is moderate. Even if it is not, the impact on the heat transfer coefficient should be negligible for gas cooling (heat recovery) applications as long as boundary layers remain laminar [30]. As regards the pressure drop, it is common practice to perform measurements in separate, adiabatic, experiments. Hence, the numerical simulations are representative of the experimental setup in this regard. Some thermal-hydraulic correlations indeed correct for the direction of heat flow, but to verify such dependencies is outside the scope of this paper.

The fins are modeled using an isotropic conducting material with constant thermal conductivity corresponding to carbon steel ($48.5\,\mathrm{W\,m^{-1}\,K^{-1}}$), aluminum ($193\,\mathrm{W\,m^{-1}\,K^{-1}}$) or copper ($375\,\mathrm{W\,m^{-1}\,K^{-1}}$), matching the experimental setup.

3.3. Full tube bundle model

The computational domain and boundary conditions for the full tube bundle model are indicated schematically in Figure 2. A single fin pitch is modeled in the spanwise direction (not shown), using periodic boundary conditions, following [17]. A uniform profile for velocity, temperature and modified turbulent viscosity is prescribed on the inlet, with a Neumann condition for pressure. Conversely, pressure in prescribed on the domain outlet.

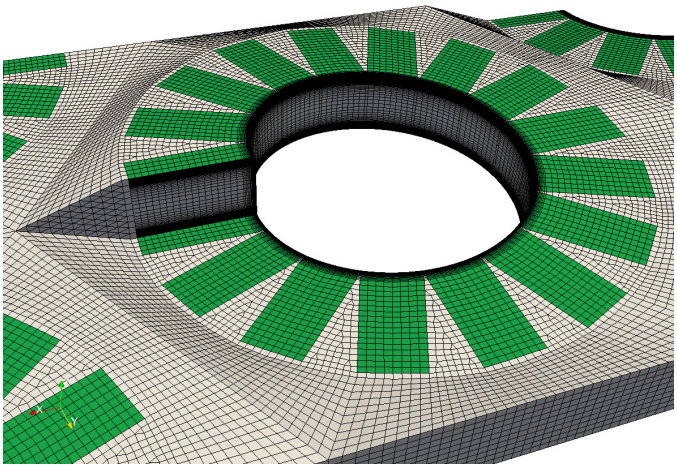

Figure 4: Computational grid example; Fully serrated fin, fin domain colored green, bulk fluid cell size is enlarged for clarity

3.4. Reduced domain model

The reduced domain (depicted in Figure 3) uses a prescribed velocity profile on the leftmost ("inflow") boundary and a prescribed pressure profile on the rightmost ("outflow") boundary, with Neumann conditions for pressure and velocity, respectively. The profiles are updated regularly during the solution process by sampling from the opposing patch, in a staggered fashion, to avoid numerical instability. The profiles for temperature and modified turbulent viscosity are updated every iteration, acting as a fully periodic boundary. Uniform profiles are used initially. The number of iterations between profile updates are adjusted to ensure convergence. In addition to being copied, profiles for velocity and temperature are scaled to satisfy a specified area average, such that flow rate and temperature difference can be set. Simulations are considered converged when total pressure drop and surface heat fluxes does not change significantly between profile updates, nor with continued iterations.

3.5. Grid generation and grid convergence study

A hexahedra-dominated hybrid grid is generated around the fin-tubes consisting of a boundary-layer resolving grid in the fluid gap between the fins and an approximately uniform grid for the bulk fluid between the fin tubes. Polyhedral cells are used to connect the two mesh regions. This ensures a consistent resolution of the inter-fin flow, with $y^+ < 1$ and

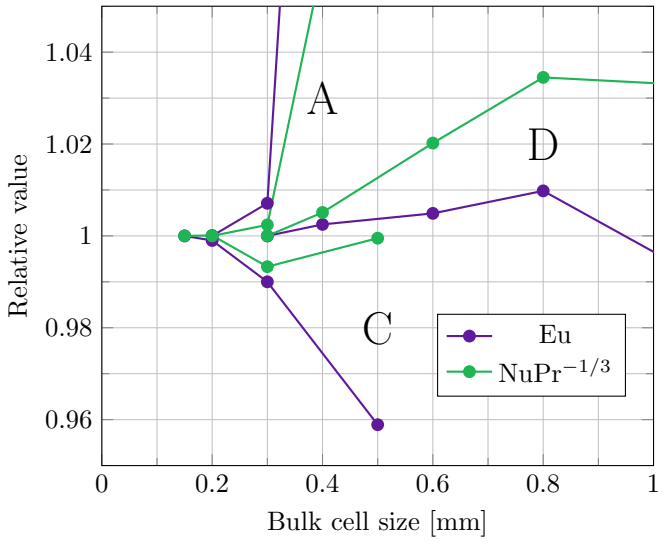

Figure 5: Grid convergence for fin-tube geometries A, C and D

a sufficient number of cells in the boundary layer, for all bulk fluid cell sizes. A typical computational grid is shown in Figure 4. The asymmetric geometry of the helically wound fin is accurately represented, which is believed to be important for an accurate pressure drop prediction.

Grid convergence is tested on the reduced computational domain for three of the fin-tube geometries (A, C and D). The bulk fluid resolution is varied while keeping the boundary layer growth rate and wall y^+ constant. Euler and Nusselt numbers are generally found to be within $\pm 1\,\%$ of its asymptotic value at a bulk cell size of 0.3 mm, as shown in Figure 5. A cell size of 0.4 mm is judged acceptable for the largest fin-tube, but it is interesting to note that the resolution requirement does not scale with the tube or fin dimensions. The boundary layer growth rate was varied independently for one of the tube geometries as an additional test. Comparing simulations with a 7 % growth and a 20 % growth rate revealed differences in Euler and Nusselt numbers of less than 0.1 %. Hence, a boundary layer cell growth rate of 20 % was used throughout for production simulations. Adiabatic boundary conditions were used for fin tips and segment sides in the grid convergence tests.

4. Data reduction

Upon convergence, the raw data from the numerical model (T,p,U,... fields) is integrated and reduced to Nusselt, Euler and Reynolds numbers to facilitate interpretation and comparison with correlations. *Average* Nusselt and Euler numbers are calculated for the full tube bundle simulation, whereas local numbers are calculated for the single central tube in the reduced domain case.

The temperature and pressure fields of the fluid are mass flow averaged before and after the fin-tube bundle as a basis for the data reduction. The inflow and outflow boundaries are used for this purpose in the full domain case. For the reduced domain, mass flow averaging planes are inserted before and after the central fin-tube, as indicated in Figure 3, to compute the drop in total pressure ($p_0 + 1/2\rho U^2$). Mass flow averaging planes are also inserted in the full domain model for comparison with the data reduction of the reduced domain model.

The wall heat flux from the active heat transfer area is evaluated numerically based on Fourier's law and the near-wall fluid temperature gradient. The bulk temperatures used in heat flux normalization are then computed from the inlet temperature plus the per-row temperature change to ensure consistency, viz.

$$T_{b,i} = T_{b,\mathrm{in}} + \frac{\sum_{n=1}^{n=i-1} \dot{Q}_{w,n}}{\dot{m} c_{p,m}} \tag{1}$$

for tube row index $i \in \{1, \ldots, N_r + 1\}$. For reduced domain cases, $T_{b,\mathrm{in}}$ is the bulk temperature on the periodic inlet.

The heat transfer coefficient is calculated as

$$\alpha_o = \frac{\dot{Q}_f + \dot{Q}_t}{[\eta_f A_f + A_t]\Delta T} \tag{2}$$

where, in the full tube bundle simulation, η_f is the area average fin efficiency and ΔT is the log mean temperature difference,

$$\Delta T = \frac{(T_{b,\mathrm{in}} - T_t) - (T_{b,\mathrm{out}} - T_t)}{\ln(T_{b,\mathrm{in}} - T_t) - \ln(T_{b,\mathrm{out}} - T_t)} \tag{3}$$

The reduced domain cases uses the arithmetic temperature difference (since no counter-flow occurs in a single tube row),

$$\Delta T \approx \Delta T_{\mathrm{A}} = \frac{1}{2}((T_{b,\mathrm{before}} - T_t) + (T_{b,\mathrm{after}} - T_t)) \tag{4}$$

where $T_{b,\mathrm{before}}$ and $T_{b,\mathrm{after}}$ are bulk temperatures before and after the central tube, respectively.

The fin efficiency is evaluated from the computed fin surface temperature field,

$$\eta_f = \frac{\dot{Q}_{\mathrm{actual}}}{\dot{Q}_{\mathrm{ideal}}} = \frac{\alpha_o \int_{\mathrm{fin}} (T_b - T_f)\,\mathrm{dA}}{\alpha_o A_f (T_b - T_t)} = \frac{T_b - T_{f,\mathrm{avg}}}{T_b - T_t} \tag{5}$$

where $T_{f,\mathrm{avg}}$ is the area-averaged temperature of the fin, viz.

$$T_{f,\mathrm{avg}} = \frac{1}{A_f} \int_{\mathrm{fin}} T_f\,\mathrm{dA} \tag{6}$$

The heat transfer coefficient is normalized by the outer diameter of the tubes, and the fluid properties, forming

$$\mathrm{NuPr}^{-1/3} = \frac{d_o \alpha_o}{k} \left(\frac{c_p \mu}{k}\right)^{-1/3} \tag{7}$$

The Reynolds number is correspondingly defined as

$$\mathrm{Re} = \frac{d_o u_{F_{\min}}}{\nu} \tag{8}$$

The pressure drop is normalized by the velocity head in the minimum free flow area $\frac{1}{2}\rho u^2_{F_{\min}}$, viz

$$\mathrm{Eu} = \frac{\Delta p}{\frac{1}{2}\rho u^2_{F_{min}} N} = \frac{\rho \Delta p}{\frac{1}{2}\dot{m}''^2 N} \tag{9}$$

where N is the number of tube rows that Δp is calculated over.

Finally, the theoretical and corrected fin efficiencies are needed for later comparison with the numerically integrated one (Equation 5). An iterative method is needed to find the theoretical, and the corrected theoretical, fin efficiency from the raw simulation data (Q_f, Q_t, A_f, A_t, ΔT). This is a result of the implicit equation for the outer heat transfer coefficient:

$$\alpha_o = \frac{\dot{Q}_f + \dot{Q}_t}{\left[\eta_{f,\mathrm{theo}}(\alpha_o, d_o, h_f, \dots) A_f + A_t\right] \Delta T} \tag{10}$$

This equation can be solved by back-substitution, i.e. by guessing an outer heat transfer coefficient, calculating the fin efficiency, and then updating α_o and η_f in succession until convergence. Note, therefore, that each method of calculating η_f corresponds to a unique α_o, since the transferred heat and ΔT remain constant.

5. Results and discussion

5.1. Full domain versus reduced domain model

Figure 6 shows a comparison between the Nusselt and Euler numbers of the full tube bundle model, the reduced domain model and experimental data for tube bundle C. It is clear that the reduced domain model gives near identical results compared to the full tube bundle model, at a much reduced computational cost. The small differences between the models can be attributed to the different expressions for ΔT used in data reduction as well as tube bundle entry and exit effects.

Figure 7 shows the pressure profile in the full tube bundle model, including entry and exit effects. The slope of the actual pressure curve, taken between two points spaced one tube row apart, matches well with the average pressure curve after the first tube row. This confirms earlier indications that the reduced model is representative of the full tube model after (at least) the third tube row [18] and that a data reduction method using mass averaged pressure planes to compute the Euler number is acceptable.

The computational cost for the reduced domain model was approximately one-seventh of that of the full domain model, which reflects the difference in the physical size of the domain as well as the faster convergence of the reduced model. The differences in model sizes and solution times for all cases are shown in Table 2.

5.2. Predictive accuracy of CFD

Nusselt and Euler numbers predicted by the reduced domain numerical model are compared to experimental data and reference correlations in Figures 8 to 11. In general, numerical model predictions are either within or close to the experimental uncertainty region of all four fin-tube geometries. The largest root mean square errors are 13.8 % for heat transfer (Geometry A) and 14.4 % for pressure drop (Geometry C). These errors are likely the result of inaccurate geometric representation (e.g. failure to model segment fin tip twist, burr edges and weld fillets) and/or turbulence model errors. No major difference can be seen in the prediction accuracy of plan fins versus that of serrated fins. This is encouraging, given the more complex flow around serrated fins, with repetitive boundary layer breakup and fluid mixing.

5.3. Thermal-hydraulic correlation accuracy

A few interesting trends can be noted regarding the predictive accuracy of the selected thermal-hydraulic correlations. The Holfeld correlations are clearly the superior equation set for predicting heat transfer for the investigated geometries. The ESCOA correlations for heat transfer perform poorly for the three small-diameter geometries, with errors of around 50 %. The PFR correlations perform relatively well given their simplicity, but relatively large errors are seen for geometry C. Notably, the three heat transfer correlations agree well for the large diameter tube.

The pressure drop predictions show a different trend than the heat transfer predictions. Overall, the PFR correlation gives best predictions, with the Holfeld correlations being moderately more in error for geometry B. The ESCOA correlations again err significantly or the non-conservative side, particularly for the serrated fin tubes. The three pressure drop correlation sets agree more for the small diameter tubes compared to the large diameter one.

5.4. Fin efficiency correction accuracy

Figure 12 shows a comparison between the numerically integrated fin efficiency and the two selected fin efficiency correction equations. For geometry A, the actual (numerical) fin efficiency is quite close to the theoretical one ($\eta_f/\eta_{f,\mathrm{theo}} = 1$), even at high Reynolds numbers, indicating that a correction is largely unnecessary. The two proposed correction equations are indeed further away from the numerically integrated one, and hence detract from modeling accuracy. The unusual ratio between fin height and tube diameter of geometry A can explain this discrepancy.

Contrary to geometry A, the actual fin efficiency of geometry C and D is substantially lower than what the theoretical fin efficiency model predicts. The Weierman correction offers significant improvement over the theoretical model, although an even stronger correction would be needed in these cases to fully compensate for the non-uniform heat transfer coefficient.

The Hashizume correction degrades accuracy for all considered cases, and indeed has a slope inconsistent with the data from the numerical models. In fairness, it should be noted that all three geometries violate the validity ranges

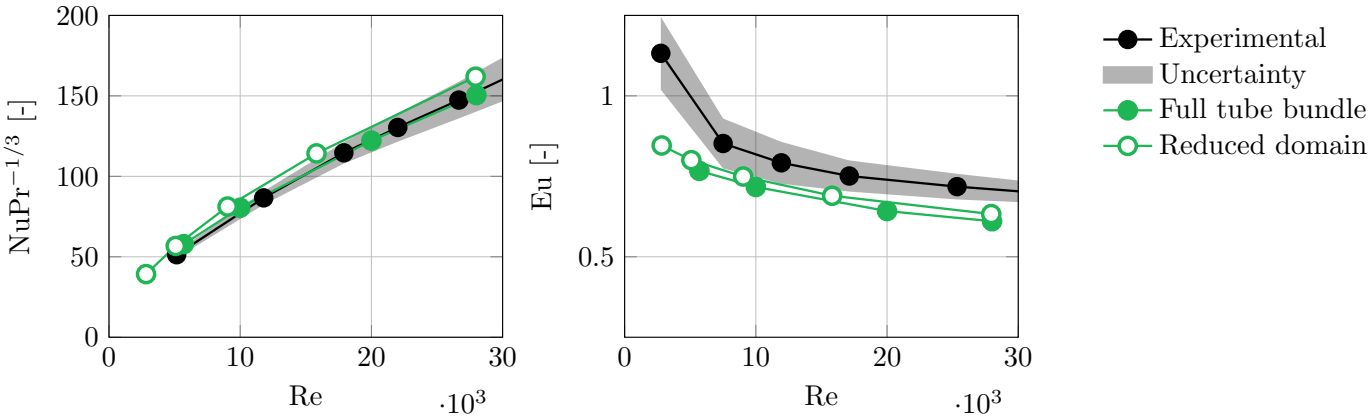

Figure 6: Full versus reduced domain, geometry C

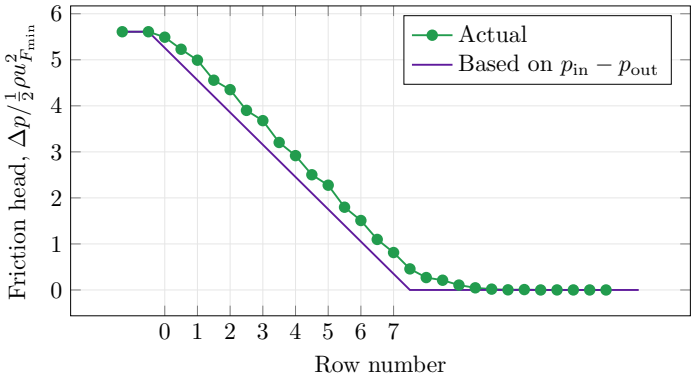

Figure 7: Mass averaged pressure change through the full tube bundle model

of the Hashizume equation slightly, but the correction nonetheless appear excessively strong.

6. Conclusions

This paper has presented a numerical model of solid and serrated fin-tube bundles, compared results to experimental data as well as semi-empirical correlations and used the numerically calculated fin temperature distribution to evaluate fin efficiency models. The following conclusions are drawn:

- RANS-based simulations can predict the thermal-hydraulic performance of fin-tube bundles with good accuracy for a range of helically wound solid- and serrated-fin geometries, provided that best practice grid generation guidelines are followed and that grid convergence is demonstrated
- Numerical simulations enable time efficient and consistent parameter studies, particularly when geometric periodicity can be exploited
- Compared to empirical correlations, the heat transfer results are consistent with the recent Holfeld correlation for the selected geometries. There is considerable inconsistencies between the correlations for pressure drop, and no single correlation capture the numerical predictions for all geometries.
- Access to the local fin temperature distribution enables fin efficiency evaluations which would have been quite tedious to perform experimentally.
- In general, the fin efficiency, calculated on the basis of a constant heat transfer coefficient, is negatively influenced by the actual uneven heat transfer coefficient distribution. The reduction in fin efficiency depends on the fin geometry and material, and the magnitude of the average heat transfer coefficient. The fin-correction correlation of Weierman captures the numerically computed trends, but does not reproduce the numerical values. Clearly, more work is required in this area.

Numerical simulations are well suited to perform broader parameter studies in future work, in order to identify the exact applicability limits of current correlations and suggest areas where further experimental work is needed. Simulations will also continue to have an important role in the heat exchanger design process, in addition to correlations and experimental validation.

Table 2: Grid size and computational cost comparison; all simulations performed on a compute cluster based on Intel Xeon E5-2670 processors

Geometry	A	B	C		D
Modeled domain	reduced	reduced	full	reduced	reduced
Inter-tube cell size [mm]	0.20	0.20	0.20	0.20	0.40
Fluid domain cell count [$\cdot 10^6$]	4.21	1.28	15.36	3.70	5.68
Solution time [CPU-hr]	331	136	2355	327	148

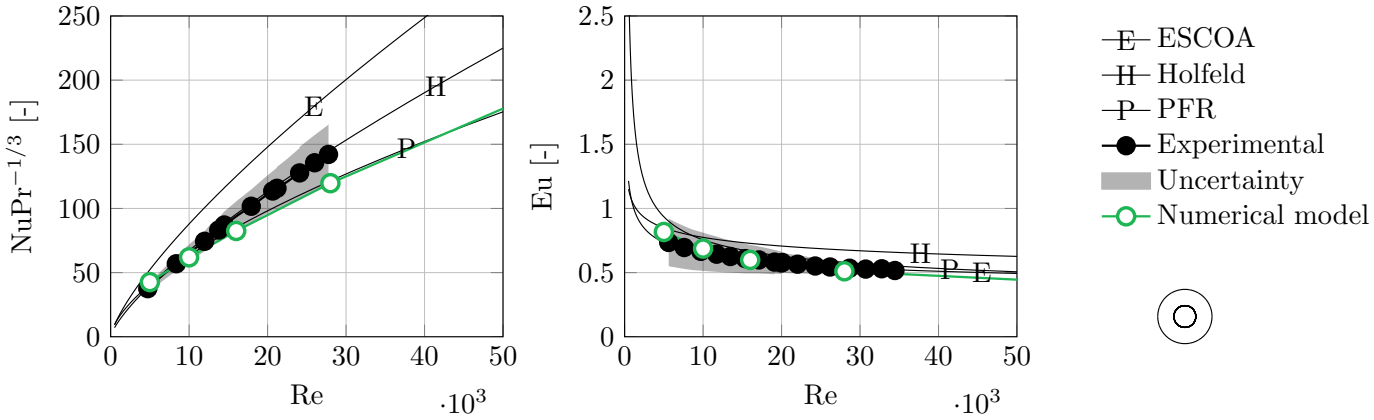

Figure 8: Thermal-hydraulic results, Geometry A; Experimental data and uncertainty from [21]

Acknowledgment

The authors acknowledge the partners: Neptune Energy Norge AS, Alfa Laval, Statoil, Marine Aluminium, NTNU, SINTEF and the Research Council of Norway, strategic Norwegian research program PETROMAKS2 (#233947) for their support.

Nomenclature

A_f	fin heat transfer area [m^2]
A_t	tube heat transfer area [m^2]
d_o	outer tube diameter [m]
$F_{\min}$	minimum free flow area [m^2]
h_f	total fin height [m]
h_s	segmented height [m]
m	nondimensional fin parameter [-]
$\dot{m}$	mass flow [kg s^{-1}]
$\dot{m}''$	mass flux ($= \dot{m}/F_{\min}$) [kg s^{-1} m^{-2}]
N	number of tube rows [-]
p	total pressure [Pa]
p_0	static pressure [Pa]
P_t	transverse tube pitch [m]
P_l	longitudinal tube pitch [m]
$\dot{Q}$	heat flow [W]
s_f	fin pitch [m]
$\hat{s}_f$	fin aperture ($= s_f - t_f$) [m]
T	temperature [K]
t_f	fin thickness [m]
$u_{F_{min}}$	mean velocity in minimum free flow area [m s^{-1}]
w_s	segment width [m]
y^+	nondimensional wall distance [-]

Greek symbols

α_o	external heat transfer coefficient [W m^{-2} K^{-1}]
α_e	apparent heat transfer coefficient [W m^{-2} K^{-1}]
β	tube bundle layout angle [°]
η_f	fin efficiency [-]
$\tilde{\nu}$	modified turbulent viscosity [m^2 s^{-1}]

Subscripts

avg	average
b	bulk, mixing cup
f	fin
t	tube
theo	theoretical

References

[1] G. Skaugen, H. T. Walnum, B. A. L. Hagen, D. P. Clos, M. Mazzetti, P. Nekså, Design and optimization of waste heat recovery unit using carbon dioxide as cooling fluid, in: Proceedings of the ASME 2014 Power Conference, 2014, pp. 1–10.

[2] A. Holfeld, E. Næss, Influence of the Fin Type and Base Tube Diameter of Serrated and Solid-Fin Tubes on the Heat Transfer and Pressure Drop Performance, in: Proceedings of the 15th International Heat Transfer Conference, IHTC-15, 1, Tokyo, Japan, 2014, pp. 1–12.

[3] M. S. Mon, Numerical investigation of air-side heat transfer and pressure drop in circular finned-tube heat exchangers, Ph.D. thesis, Technischen Universität Bergakademie Freiberg, 2003.

[4] P. Stephan, S. Kabelac, M. Kind, H. Martin, D. Mewes, K. Schaber, VDI Heat Atlas, Springer Berlin Heidelberg, Berlin, Heidelberg, 2010.

[5] M. S. Mon, U. Gross, Numerical study of fin-spacing effects in annular-finned tube heat exchangers, International Journal of Heat and Mass Transfer 47 (2004) 1953–1964.

[6] R. K. Banerjee, M. Karve, J. H. Ha, D. H. Lee, Y. I. Cho, Evaluation of Enhanced Heat Transfer Within a Four Row Finned

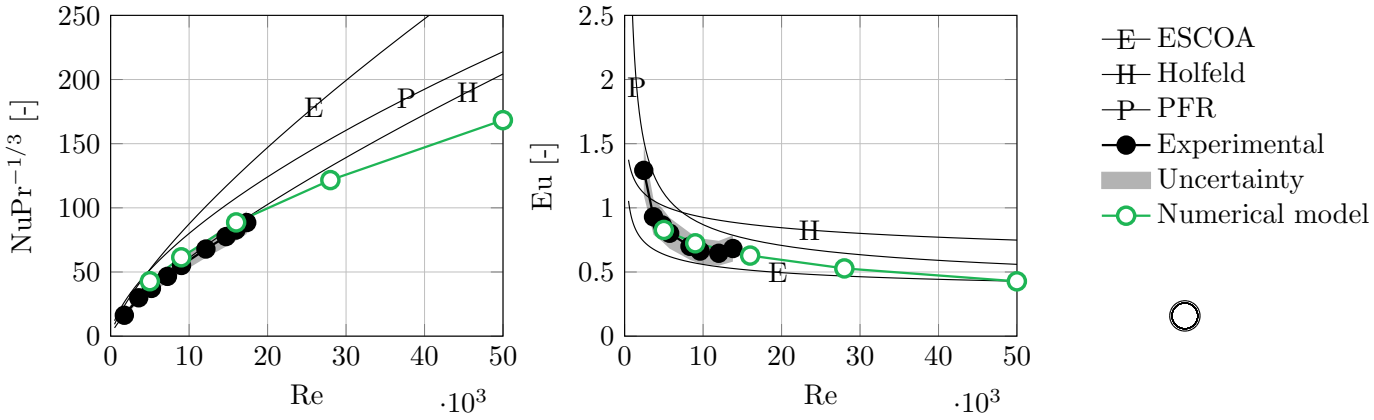

Figure 9: Thermal-hydraulic results, Geometry B; Experimental data from [22], estimated uncertainty

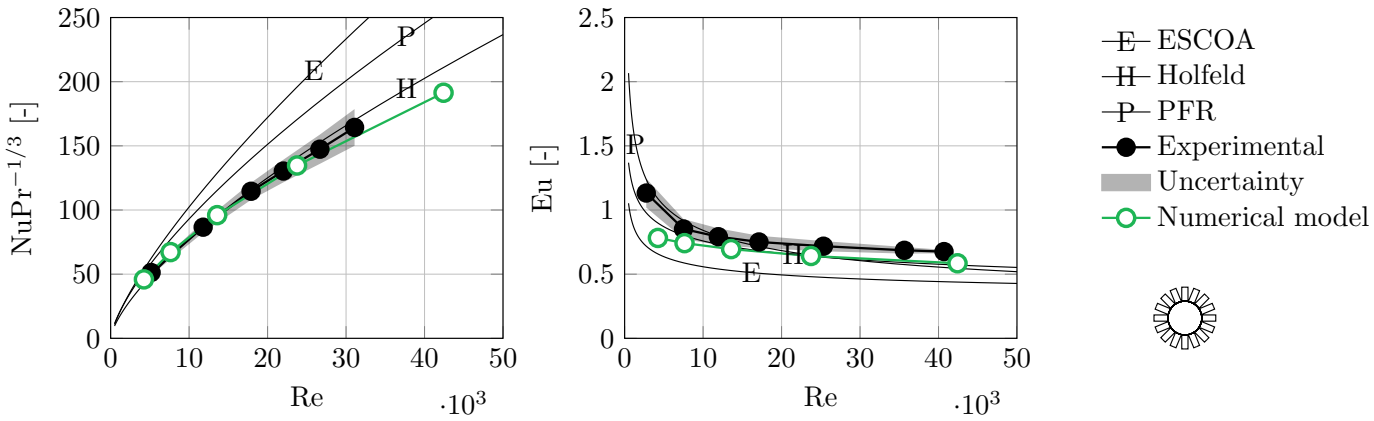

Figure 10: Thermal-hydraulic results, Geometry C; Experimental data and uncertainty from [23]

Tube Array of an Air Cooled Steam Condenser, Numerical Heat Transfer, Part A: Applications 61 (2012) 735–753.

[7] H. Bilirgen, S. Dunbar, E. K. Levy, Numerical modeling of finned heat exchangers, Applied Thermal Engineering 61 (2013) 278–288.

[8] S. Pathak, K. Velusamy, K. Rajan, C. Balaji, Numerical and experimental investigations of heat removal performance of sodium-to-air heat exchanger used in fast reactors, Heat Transfer Engineering 36 (2015) 439–451.

[9] S. R. McIlwain, Improved Prediction Methods for Finned Tube Bundle Heat Exchangers in Crossflow, Ph.D. thesis, University of Strathclyde, 2003.

[10] M. Torresi, A. Saponaro, S. M. Camporeale, B. Fortunato, CFD Analysis of the Flow Through Tube Banks of HRSG, in: Proceedings of ASME Turbo Expo 2008, Berlin, Germany, 2008, pp. 1–11.

[11] S. R. McIlwain, A Comparison of Heat Transfer Around a Single Serrated Finned Tube and a Plain Finned Tube, International Journal of Research & Reviews in Applied Sciences 2 (2010) 88–94.

[12] S. R. McIlwain, A CFD Comparison of Heat Transfer and Pressure Drop Across Inline Arrangement Serrated Finned Tube Heat Exchangers With an Increasing Number of Rows, International Journal of Research & Reviews in Applied Sciences 4 (2010) 162–169.

[13] R. Hofmann, Experimental and Numerical Air-Side Performance Evaluation of Finned-Tube Heat Exchangers, Ph.D. thesis, Technischen Universität Wien, 2009.

[14] R. Hofmann, H. Walter, Experimental and Numerical Investigation of the Gas Side Heat Transfer and Pressure Drop of Finned TubesPart I: Experimental Analysis, Journal of Thermal Science and Engineering Applications 4 (2012) 041007.

[15] R. Hofmann, H. Walter, Experimental and Numerical Investigation of the Gas Side Heat Transfer and Pressure Drop of Finned TubesPart II: Numerical Analysis, Journal of Thermal Science and Engineering Applications 4 (2012) 041008.

[16] A. Lemouedda, A. Schmid, E. Franz, M. Breuer, A. Delgado, Numerical investigations for the optimization of serrated finned-tube heat exchangers, Applied Thermal Engineering 31 (2011) 1393–1401.

[17] C. T. Ó Cléirigh, W. J. Smith, Can CFD accurately predict the heat-transfer and pressure-drop performance of finned-tube bundles?, Applied Thermal Engineering 73 (2014) 681–690.

[18] E. Martinez, W. Vicente, M. Salinas-Vazquez, I. Carvajal, M. Alvarez, Numerical simulation of turbulent air flow on a single isolated finned tube module with periodic boundary conditions, International Journal of Thermal Sciences 92 (2015) 58–71.

[19] E. Martinez-Espinosa, W. Vicente, M. Salinas-Vazquez, I. Carvajal-Mariscal, Numerical Analysis of Turbulent Flow in a Small Helically Segmented Finned Tube Bank, Heat Transfer Engineering 38 (2017) 47–62.

[20] E. Martinez-Espinosa, W. Vicente, M. Salinas-Vazquez, Numerical Analysis for Saving Fin Material in Helical Segmented-Tubes, Applied Thermal Engineering 110 (2017) 306–317.

[21] A. Holfeld, Experimental investigation of heat transfer and pressure drop in compact waste heat recovery units, Ph.D. thesis, Norwegian University of Science and Technology, 2016.

[22] D. J. Ward, E. H. Young, Heat transfer and pressure drop of air in forced convection across triangular pitch banks of finned tubes, Chem. Eng. Progr. 55 (1959).

[23] E. Næss, Experimental investigation of heat transfer and pressure drop in serrated-fin tube bundles with staggered tube layouts,

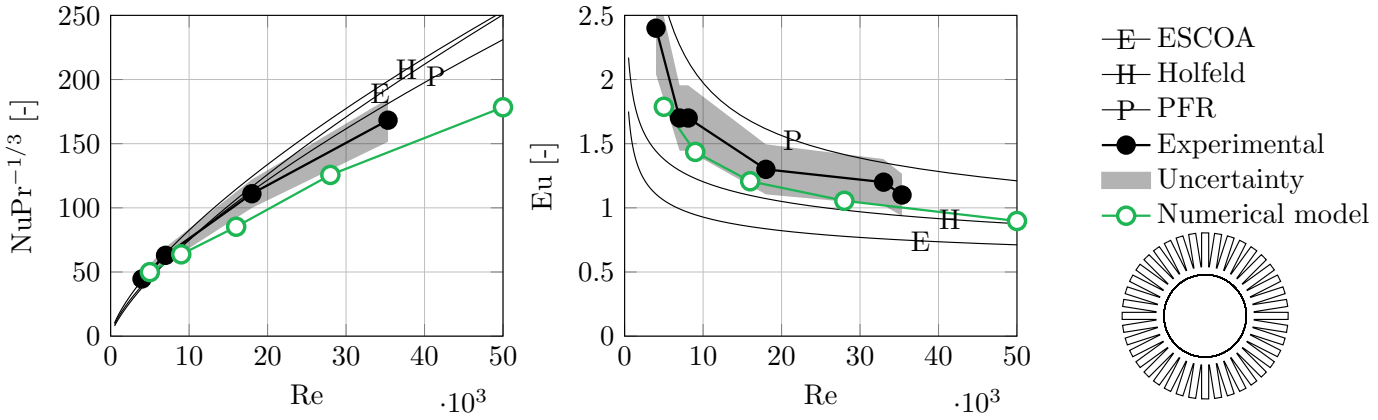

Figure 11: Thermal-hydraulic results, Geometry D; Experimental data from [24], estimated uncertainty

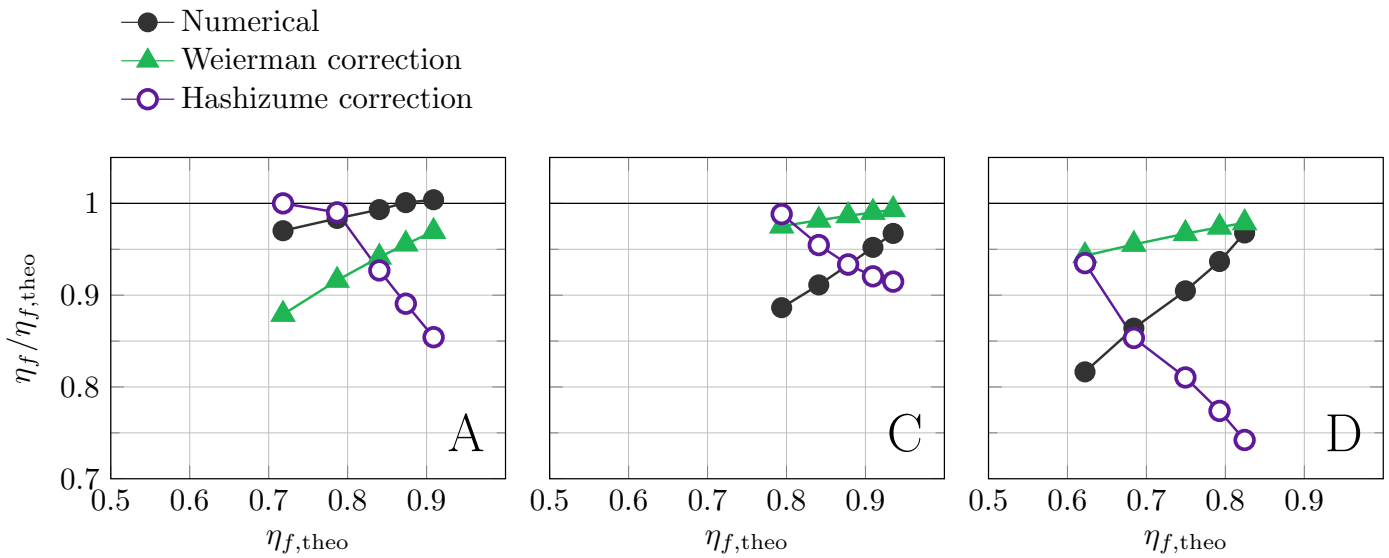

Figure 12: Fin efficiency correction equations compared to exact fin efficiency from numerical simulations for fin-tube geometries A, C and D.

Applied Thermal Engineering 30 (2010) 1531–1537.

[24] C. Weierman, J. Taborek, W. J. Marner, Comparison of the Performance of In-line and Staggered Banks of Tubes With Segmented Fins, AlChE Symposium Series 74 (1978) 39–46.

[25] PFR Engineering Systems Inc., Heat Transfer and Pressure Drop Characteristics of Dry Tower Extended Surfaces, Technical Report, PFR Report BNWL-PFR-7-100, 1976.

[26] ESCOA Fintube Corp., ESCOA Engineering Manual (electronic version), Technical Report, Downloaded September 2005 from http://www.fintubetech.com/escoa/, 2002.

[27] C. Weierman, Correlations ease the selection of finned tubes, Oil Gas J 74 (1976) 10–94.

[28] K. Hashizume, R. Morikawa, T. Koyama, T. Matsue, Fin Efficiency of Serrated Fins, Heat Transfer Engineering 23 (2002) 6–14.

[29] H. Nemati, M. Moghimi, Numerical Study of Flow Over Annular-Finned Tube Heat Exchangers by Different Turbulent Models, CFD Letters 6 (2014).

[30] W. M. Kays, M. E. Crawford, B. Weigand, Convective Heat and Mass Transfer, fourth edi ed., McGraw-Hill Education, New York, 2005.